

EVALUATION OF FORMABILITY OF THIN SHEETS BASED ON Al-Mg-Si FOR AUTOMOTIVE INDUSTRY

Patrik Petroušek^{1)*}, Tibor Kvačkaj¹⁾, Róbert Kočíško¹⁾, Róbert Bidulský¹⁾, Jana Bidulská¹⁾, Alica Fedoriková¹⁾, Tomáš Hlava²⁾

¹⁾ Technical University of Košice, Faculty of Metallurgy, Košice, Slovakia

²⁾ MATADOR Automotive Vrábľa, a.s., Engineering Support

Received: 21.09.2015

Accepted: 29.09.2015

*Corresponding author: e-mail: patrik.petrousek@tuke.sk, Tel.: +421 55 602 4257 Department of Metals Forming, Faculty of Metallurgy, Technical University of Košice, Vysokoškolská 4, 04200 Košice, Slovakia

Abstract

In this paper is evaluated workability of rolled aluminium alloy based AlMgSi. Static tension test was used for obtained the mechanical properties, such as tensile strength, yield strength, elongation, the strain hardening exponent and coefficient of surface anisotropy. Rolled samples used for a tensile test were taken in three different directions, namely in the direction of rolling, in 45 ° and 90° direction. The result is an consideration of suitability of the material for stamping technology. For measurement of the elongation, variations in thickness and width in real-time was used method called videoextensometry. To obtain deforming maps and left side of forming limit diagrams (FLD) was applied digital correlation method (DIC).

Keywords: aluminium alloys, mechanical properties, videoextensometry, DIC method, FLD diagram

1 Introduction

Al–Mg–Si alloys or EN AW 6000 series alloys are widely used for medium strength structural applications and also in increasing demand in the automotive industry. These alloys have been the materials of choice for skin panels because they have a combination of good formability and medium strength. The alloys are age hardenable and strengthened by Mg₂Si, which is the primary hardening phase [1-4]. Mg and Si are the major solutes in these alloys, which increase the strength of the material by the formation of strengthening agents (precursors to Mg₂Si) during the paint-bake cycle [5-7].

The use of lightweight materials can help reduce vehicle weight and improve fuel economy. The pressure for weight reduction has driven a gradual decrease in the amount of steel and cast iron used in vehicles and the corresponding increase in the amount of alternative materials, especially aluminium [8-14].

Currently, the plane formability evaluation uses a number of techniques. Among the most progressive methods include non-contact method. These methods work on the principle of deformation grid. Previous methods use mechanical applied grid [10]. They had to have regular shapes and arrangements. The new grid may use the method that is applied to the surface of the sample, e.g. coated using a special spray. On the basis of the change in position of these

elements is by software, or manually evaluate the deformation. There are known two types of analysis [15-19]:

- postprocessing - manually applied grid - (software Argus, Ncorr, etc.)
- online processing analysis - method using the principle of DIC, videoextensometry, ESPI etc. - (software Aramis, HorizonVideoextensometer, StrainMaster, etc.)

The strain measurement process requires more and more accuracy; therefore various experimental techniques are developed. Non-contact techniques allow monitoring whole testing process and provide information about measured area. Often used non-contact techniques for strain measurement are videoextensometry, DIC (digital image correlation), ESPI (electronic speckle pattern interferometry), etc [20,21].

The DIC method is a optical method which is used to measure the relative spatial deformations and displacements. This method uses digital image registration technology. For image capturing is using high-speed cameras with high image resolution. This method is seen as a flexible tool that is used not only in the field of experimental mechanics [16-18].

Measuring systems which operate on the principle of DIC method have many advantages against conventional method. For example: without contact with the measured object, possibility of measuring in any position monitored area, the ability to capture non-homogeneous deformation field in all areas, the ability to direct measurement that requires numerical or analytical processing of results, application in places where it is impossible or very difficult, high accuracy displacements of individual contrast points in the monitored field [18-22].

In this paper are obtained mechanical properties, microstructure and hardness of aluminium alloy for three differently direction of rolling. Formability of aluminium alloy can be characterized through FLD diagrams. FLD diagrams may be formed by a DIC method in ARAMIS software. For monitoring deformation in real time was used videoextensometric system by HorizonVideoextensometer.

2 Experimental material and methods

As experimental material was used EN AW 6000 series aluminium alloy based AlMgSi, both in a T4 heat treatment state according to DIN EN 515. Experimental material was cold rolled to a thickness of 1,72 mm. Static tensile test was conducted in accordance with standard STN EN ISO 6892-1 on tensile machine. In the static tensile test were used static conditions and speed of equipment movement was 0.13 mm/s. A chemical composition of aluminium alloy is shown in **Table 1**.

Table 1 The local chemical analysis [mass.%]

Sample	Si	Fe	Cu	Mn	Mg	Cr	Ti	Zn	Al
Al_1,72	0,868	0,189	0,138	0,155	0,571	0,008	0,018	0,06	97,7

The samples were prepared in three different directions to the rolling direction (0° , 45° , 90°). Mechanical properties were evaluated by tensile test - yield strength ($R_{p0,2}$), ultimate tensile strength (R_m), elongation (A_{80}), strain hardening index (n), coefficient of surface anisotropy (a). To obtain the forming limit diagrams the samples needed to be prepared as shown as in the **Fig. 1**. On the specimens were created five different notches in the central portion. The shape was designed that the plastic deformation was concentrated in the centre of the sample. Black stochastic spotted image was created using a special graphite-spray on a white background. The authors [23,24] developed a methodology of software ARAMIS.

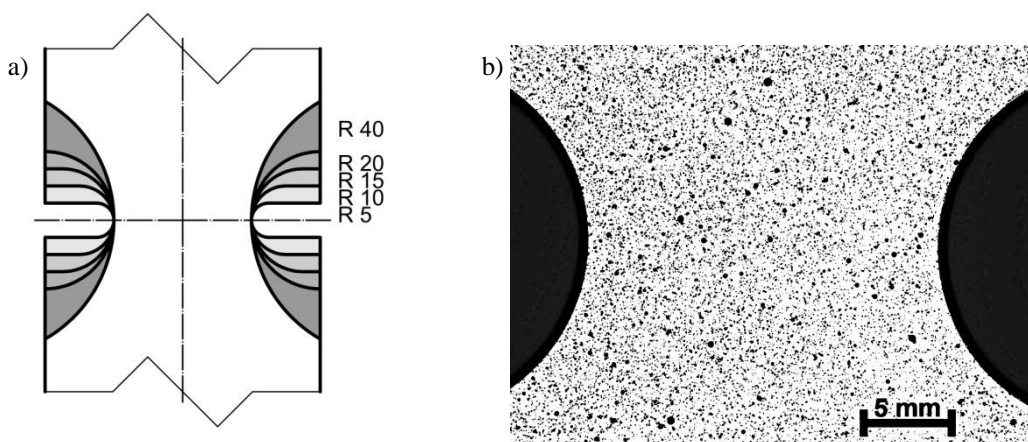


Fig. 1 Samples for FLD measuring: a) schematic representation [in mm] ; b) black stochastic spotted image

3 Results

In **Fig. 2** and **Fig. 3** is shown the microstructure of aluminium alloy in direct and perpendicular direction. The directions 0° and 90° are boundary conditions. The microstructure in a straight line is elongated in the rolling direction. Within the grains of the second phase are particles which are made up of Mg_2Si .

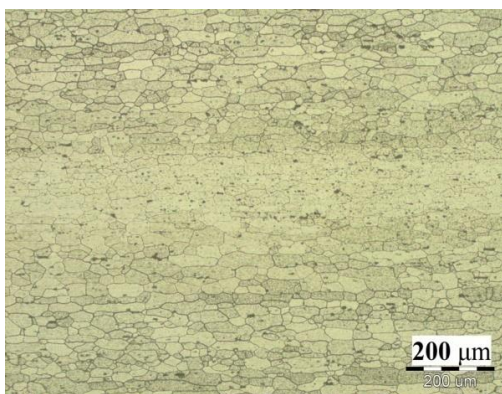


Fig. 2 Microstructure of direction 0°

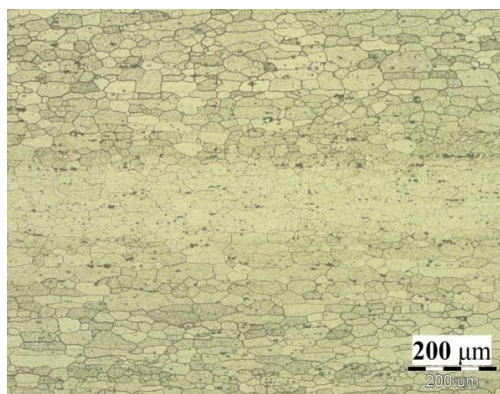


Fig. 3 Microstructure of direction 90°

The **Fig. 4** is a graphical dependence of $Rp_{0.2}$, Rm and ratio $Rp_{0.2}/Rm$ according to the direction of sampling. The highest values of $Rp_{0.2}$ and Rm were obtained on the samples taken at angle of 0° (in rolling direction). The lowest values of $Rp_{0.2}$ and Rm are approximately the same of direction at angle 45° and 90° . The ratio $Rp_{0.2}$ and Rm in all directions exhibits little change.

The **Fig. 5** shows a plot of elongation and the strain hardening exponent according to the direction of sampling. The strain hardening exponent was determined from 5% strain according to ISO 10275:2007. Based on the picture it can be stated that the elongation was approximately the same in all samples. The strain hardening was the lowest in samples taken at an angle of 0° , namely 0,2.

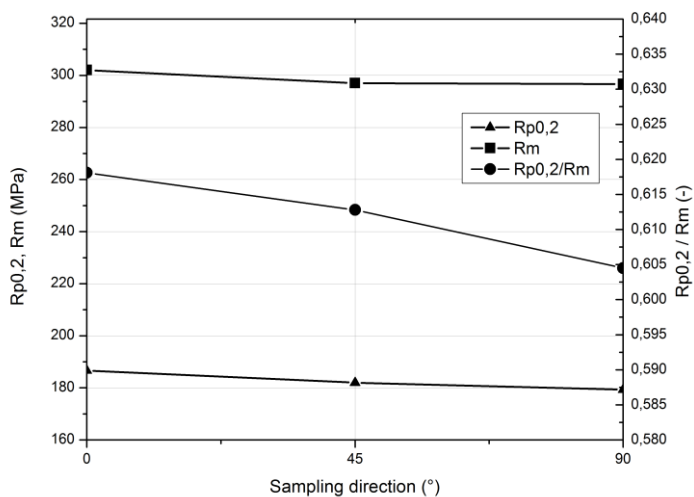


Fig. 4 The dependence of $R_{p0,2}$, R_m and ratio $R_{p0,2}/R_m$ to the direction of sample

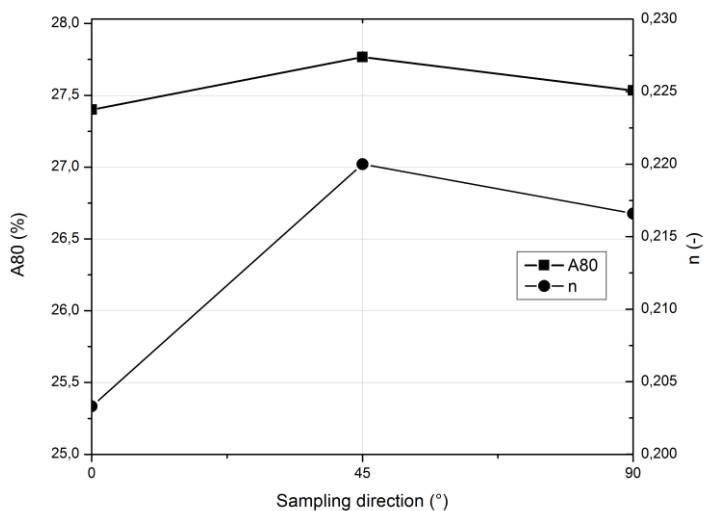


Fig. 5 The dependence of elongation and strain hardening exponent to the direction of sample

The **Table 2** shows calculated values of surface anisotropy for two different orientations relative to the direction of 0° . The percentages show the deviations between $R_{p0,2}$, R_m , and A_{80} of the properties obtained in the rolling direction.

Table 2 The obtained values of surface anisotropy

Direction of sampling	$a_{R_{p0,2}}$ [%]	a_{R_m} [%]	$a_{A_{80}}$ [%]
0°	-	-	-
45°	-2,5	-1,66	1,33
90°	-3,93	-1,77	0,49

The **Fig. 6** is a graphical dependence of real stress - real strain curve according to the direction of sampling. Thickness and width were measured by videoextensometry in real time. Therefore, true stress and true strain was calculated. The curves processed in uniform deformation are shown in **Fig. 6**. Course of the consolidation of the individual curves is approximately the same regardless of the direction of sampling. These data are one of the most important inputs of the material properties for computer simulation of forming processes.

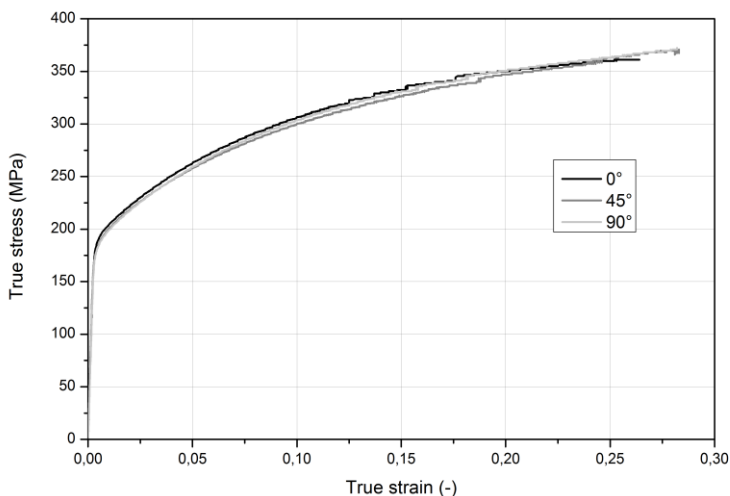


Fig. 6 The dependence of real stress – real strain to the direction of sample

In the **Fig. 7** is shown FLC curve. This curve represents the left side of the FLD diagram. These points were obtained from the area of the crack. These values represent the critical strain to cracking.

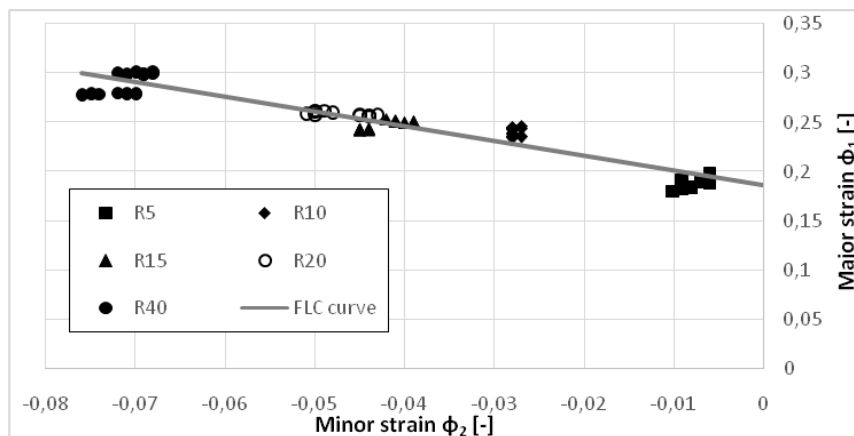


Fig. 7 FLD diagram of aluminium alloy

In the **Fig. 8**, **Fig. 9**, **Fig. 10**, **Fig. 11** are shown deformation maps for four different notch radii. When the smallest radius of cut than the rupture is is concentrates at the edge of the samples. At

the maximum radius is deformation concentrated in the centre of the sample. In the following **Fig. 8** to **Fig. 11** are evaluated deformation maps which are a functional dependence of relative major deformation.

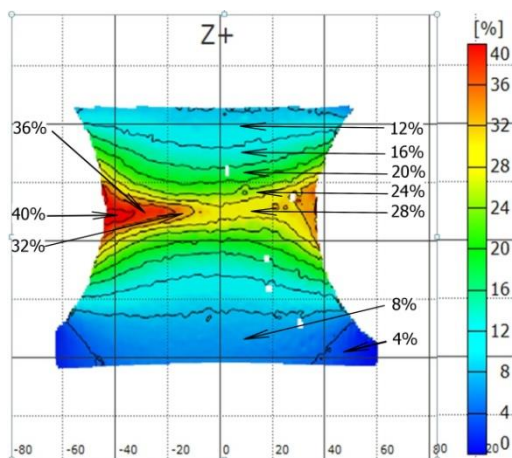


Fig. 8 Deformation maps - radius R10

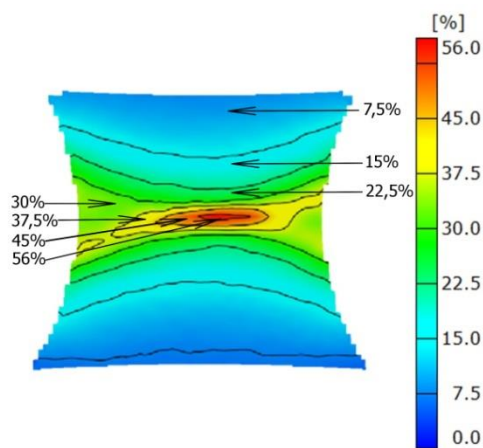


Fig. 9 Deformation maps - radius R15

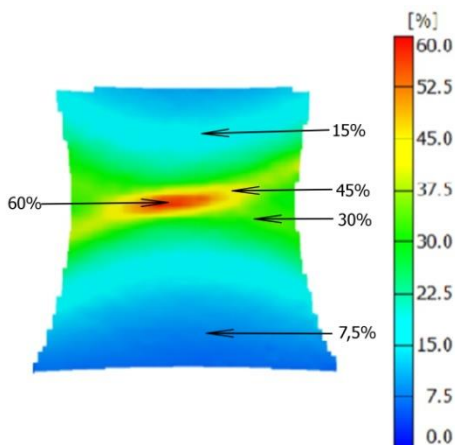


Fig. 10 Deformation maps - radius R20

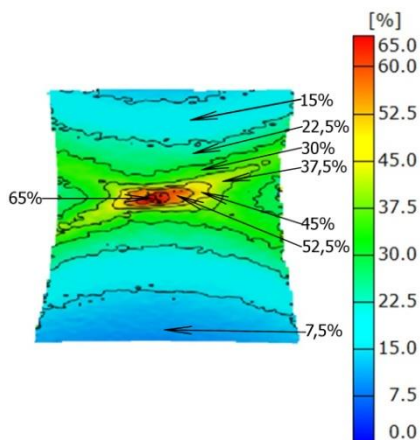


Fig. 11 Deformation maps - radius R40

Conclusions

The materials used in automobile industry offer the highest potential for improvement. Sheets of aluminium alloys can compete steels with their mechanical properties, lightweight, corrosion resistance and good formability. Based on this work, it is possible to assess the suitability of 6000 series aluminium alloy based AlMgSi for the stamping process. Based on realized experiments and measurements, achieved results can be summarized as follows:

- the direction of the sampling for this type of aluminium alloy has not significant effect on mechanical properties as documented by the coefficient of surface anisotropy (**Table 2**) and also course of curves real stress - real strain (**Fig. 6**),
- the deformation maps show the places of cracking. Here it can be seen, that with decreasing curvature of the radius is the crack focus at the edge of notch and with

increasing curvature of the radius is growing the value of deformation to failure, as illustrated by **Fig. 7**.

References

- [1] A. Jaafar et al.: *Journal of Alloys and Compounds*, Vol. 509, 2011, p. 8632-8640, DOI: 10.1016/j.jallcom.2012.12.128
- [2] J. Dutkiewicz, L.Litynska: *Materials Science and Engineering: A*, Vol. 324, 2002, No. 1-2, p. 239-243, DOI:10.1016/S0921-5093(01)01318-1
- [3] H. Liu et al.: *Transactions of Nonferrous Metals Society of China*, Vol. 17, 2007, No. 1, p. 122-127, DOI: 10.1016/S1003-6326(07)60059-4
- [4] D. Maissonette et al.: *Materials Science and Engineering: A*, Vol. 528, 2011, No. 6, p. 2718-2724, DOI: 10.1016/j.msea.2010.12.011
- [5] H. Zhong, P. Rometsch, Y. Estrin: *Transactions of Nonferrous Metals Society of China*, Vol. 24, 2014, No. 7, p. 2174-2178, DOI:10.1016/S1003-6326(14)63329-X
- [6] E. Linardi, R. Haddad, L.Lanzani: *Procedia Materials Science*, Vol. 1, 2012, p. 550-557, DOI: doi:10.1016/j.mspro.2012.06.074
- [7] A. Ambroziak, M.Korzeniowski: *Archives of Civil and Mechanical Engineering*, Vol. 10, 2010, Mo. 1, p. 5-13, DOI: 10.1016/S1644-9665(12)60126-5
- [8] W.S. Miller et al: *Materials Science and Engineering: A*, Vol. 280, 2000, No. 1, p.37-49,DOI: 10.1016/S0921-5093(99)00653-X
- [9] D.K. Koli, G. Agnihotri, R. Purohit: *Materials Today: Proceedings*, Vol. 2, 2015, No. 4-5, p. 3032-3041, DOI: 10.1016/j.matpr.2015.07.290
- [10] J. Bidulska, T. Kvacaj, R. Bidulsky, M. Actis Grande: *Acta Physica Polonica A*, Vol. 122, 2012, No. 3, p. 553-556
- [11] J. Bidulska et al.: *Chemicke Listy*, Vol. 105, 2011, No. 16, p. s471-s473
- [12] J. Bidulska et al.: *Kovove Materialy*, Vol. 46, 2008, No. 3, p. 151-155
- [13] T. Kvacaj et al.: *Archives of Metallurgy and Materials*, Vol. 58, 2013, No. 2, p. 407-412, DOI: 10.2478/amm-2013-0008
- [14] J. Bidulska et al.: *Archives of Metallurgy and Materials*, Vol. 58, 2013, No. 2, p. 371-375, DOI: 10.2478/amm-2013-0002
- [15] E. Evin, M.Tomáš, J. Kmec, S. Németh, B. Katalinic, E. Wessely: *Procedia Engineering*, Vol. 69, 2014, p. 758-767, DOI: 10.1016/j.proeng.2014.03.052
- [16] Z. Liang et al.: *Measurement*, Vol. 76, 2015, p.183-188, DOI: 10.1016/j.measurement.2015.08.026
- [17] J. Ye, S. André, L. Farge: *International Journal of Solids and Structures*, Vol. 59, 2015, p.58-72, DOI: 10.1016/j.ijsolstr.2015.01.009
- [18] P. Mazzoleni et al.. *Optics and Lasers in Engineering*, Vol. 75, 2015, p.72-80, DOI: 10.1016/j.optlaseng.2015.06.009
- [19] H. Haddadi, S.Belhabib: *International Journal of Mechanical Sciences*, Vol. 62, 2012, No. 1, p. 47-56, DOI: 10.1016/j.ijmecsci.2012.05.012
- [20] S. Hlebová, L. Ambriško, L. Pešek: *Key Engineering Materials*, Vol. 586, 2014, p. 129-132, DOI: 10.4028/www.scientific.net/KEM.586.129
- [21] G.S. Schajer, Y. Zhang, S. Melamed: *Optics and Lasers in Engineering*, Vol.67, 2015, p.116-121, DOI: 10.1016/j.optlaseng.2014.11.008
- [22] Z.F. Zhang et al.: *Measurement*, Vol. 39, 2006, p.710-718, DOI: 10.1016/j.measurement.2006.03.008

- [23] J. Karlsson et al: Materials Science and Engineering: A, Vol. 618, 2014, p. 456-461, DOI: 10.1016/j.msea.2014.09.022
- [24] F. Abbassi, S. Mistou, A. Zghal: Materials & Design, Vol. 49, 2013, p. 638-646, DOI: 10.1016/j.matdes.2013.02.020

Acknowledgements

This work was realized within the frame of the Operational Program Research and Development: "The centre of competence for industrial research and development in the field of light metals and composites", project code ITMS: 26220220154.